# Supporting Information

Triple-shelled $CuO/CeO_2$ hollow nanospheres derived from metal-organic frameworks as highly efficient catalysts for CO oxidation

Xue-Zhi Song, Qiao-Feng Su, Shao-Jie Li, Si-Hang Liu, Nan Zhang, Yu-Lan Meng, Xi Chen and Zhenquan Tan*

State Key Laboratory of Fine Chemicals, School of Chemical Engineering, Dalian University of Technology, 2 Dagong Road, Liaodongwan New District, Panjin 124221, Liaoning, P. R. China

*tanzq@dlut.edu.cn

Text S1: The detailed $H_2$-TPR+$N_2O$ experiments and TOF calculation

$H_2$ temperature-programmed reduction ($H_2$-TPR) and $N_2O$ chemisorption experiments were performed on a PCA-140 instrument. Prior to reduction, the catalyst (200 mg) was pretreated in an Ar flow (30 mL/min) from room temperature to 500 °C at a rate of 20 °C/min, and the temperature was then maintained at 500 °C for 1 h. The $H_2$-TPR+$N_2O$ chemisorption process consists of three sequential steps:

$$CuO + H_2 \rightarrow Cu + H_2O \quad (1)$$

$$2Cu + N_2O \rightarrow Cu_2O + N_2 \quad (2)$$

$$Cu_2O + H_2 \rightarrow 2Cu + H_2O \quad (3)$$

Step 1 represents the reduction of CuO in the catalysts. A flow of 5% $H_2/N_2$ (30 mL/min) was used as the reducing agent, and the temperature was increased from room temperature to 300 °C at a heating rate of 5 °C/min. The amount of $H_2$ consumption ($A_1$) corresponds to the total amount of CuO in the catalysts. Step 2 represents the oxidation of surface Cu to $Cu_2O$ by $N_2O$, which is a typical method for evaluating the dispersion and crystallite size of Cu catalysts. This step was initiated after the reduced catalyst, which was cooled to 60 °C in flowing Ar (30 mL/min) for 30 min; the catalysts were then oxidized at 60 °C for 1 h in pure $N_2O$ flowing at 30 mL/min. Subsequently, the residual $N_2O$ was removed using an Ar stream (30 mL/min) at room temperature for 1 h. Step 3 represents the reduction of $Cu_2O$ surface species. The catalysts were reduced under a 5% $H_2/N_2$ atmosphere (30 mL/min) from room temperature to 300 °C with a heating rate of 5 °C/min. The amount of $H_2$ consumed ($A_2$) corresponds to twice the amount of surface Cu in the catalyst. The dispersion ($D$) of CuO was calculated as follows:[Ref. S1]

$$D_{CuO} = 2A_2/A_1 \times 100\% \quad (4)$$

Concerning the intrinsic activity, turnover frequencies (TOFs) were calculated on the basis of the following definitions:

$$TOF(s^{-1}) = X_{CO}F_{CO}\frac{5M_{Cu}}{4m_{cat}X_{CuO}D_{CuO}} \quad (5)$$

Where $X_{CO}$ is the CO conversion at a given temperature, $F_{CO}$ is the flow rate of CO in

mol/s, $m_{cat}$ is the amount of catalyst, $X_{CuO}$ is the CuO loading in the catalyst, $D_{CuO}$ is the dispersion of CuO and $M_{Cu}$ is the molar mass of Cu (63.546 g/mol). *TOF* reflects the conventional calculation of *TOF* based on the metal dispersion.

(Ref. S1) R. Kang, X. Wei, F. Bin, Z. Wang, Q. Hao and B. Dou, Reaction mechanism and kinetics of CO oxidation over a $CuO/Ce_{0.75}Zr_{0.25}O_{2-\delta}$ catalyst. *Appl. Catal. A Gen.*, 2018, **565**, 46-58.

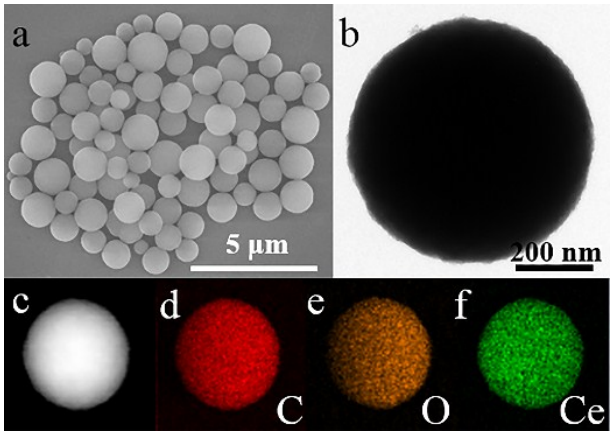


**Fig. S1** SEM image, TEM image and corresponding elemental mapping images of solid Ce-BPDC microspheres precursors.

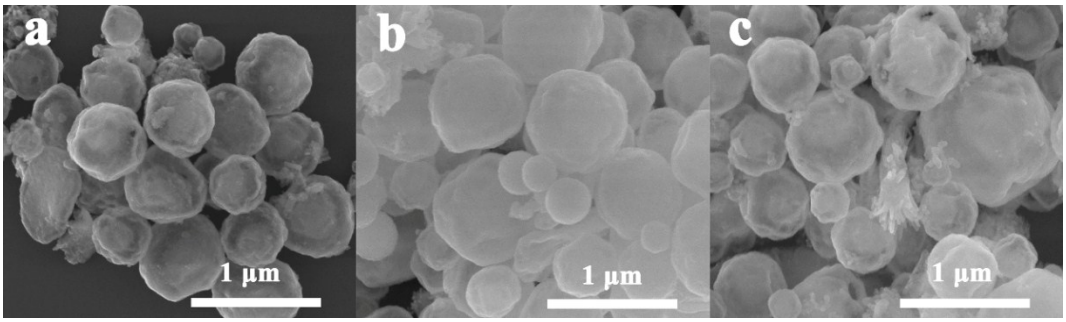


**Fig. S2** SEM images of $CuO/CeO_2$-4% (a), $CuO/CeO_2$-12% (b) and $CuO/CeO_2$-16% (c).

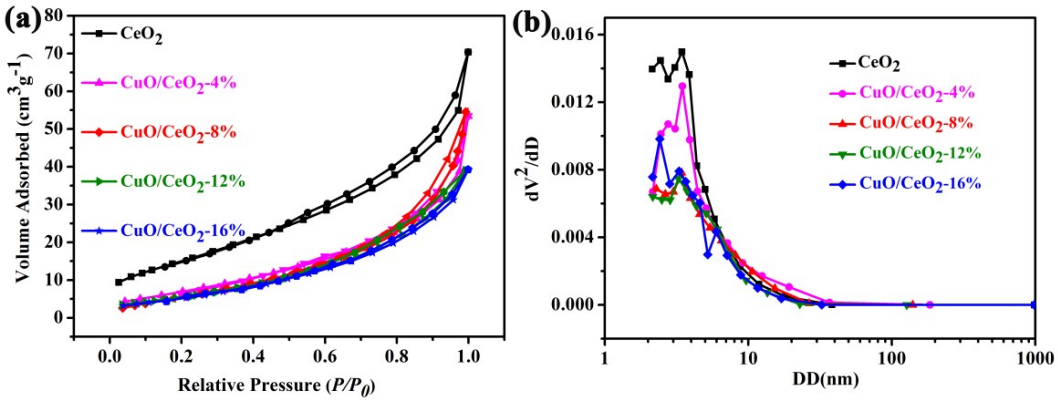


**Fig. S3** $N_2$-adsorption-desorption isotherms (a) and corresponding pore size distributions curves (b) of the $CeO_2$ support and $CuO/CeO_2$-X% samples.

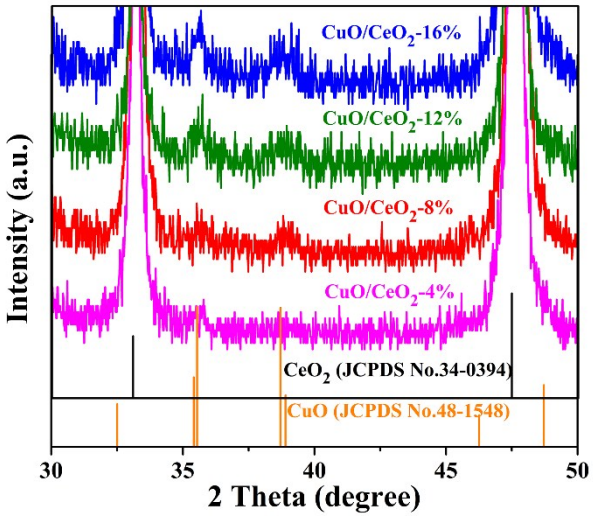


**Fig. S4** The regional magnification of XRD patterns of the support $CeO_2$ and $CuO/CeO_2$-X% samples.

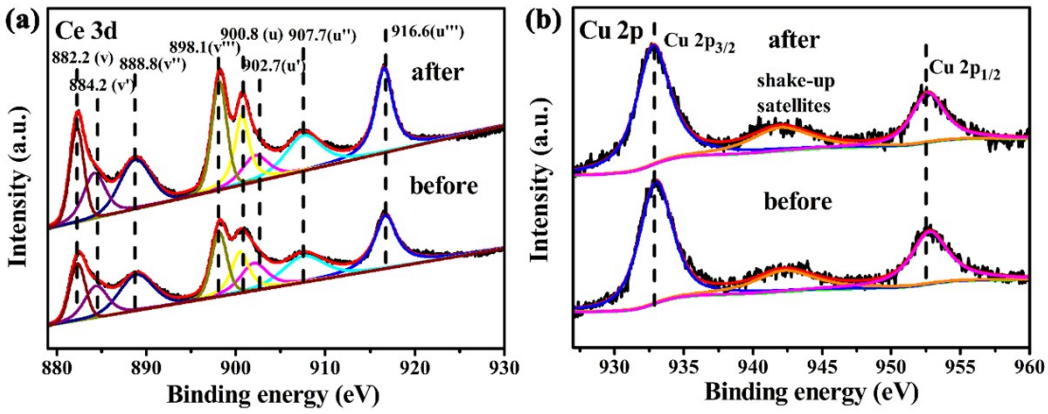


**Fig. S5** XPS spectra of Ce 3d (a) and Cu 2p (b) of the $CuO/CeO_2$-8% before and after catalysis.

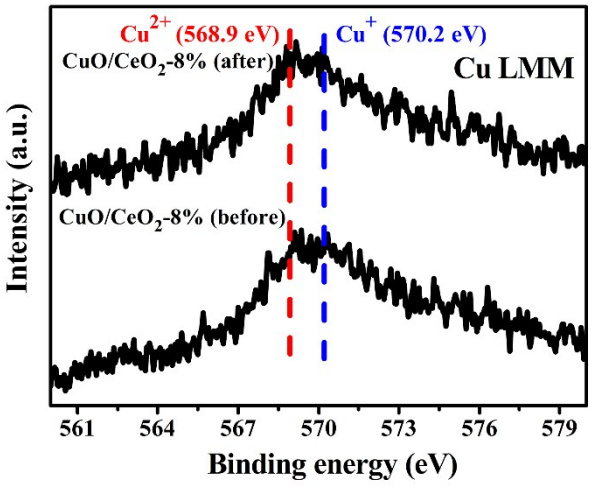


**Fig. S6** Auger lines of Cu LMM in the $CuO/CeO_2$-8% sample before and after catalysis.

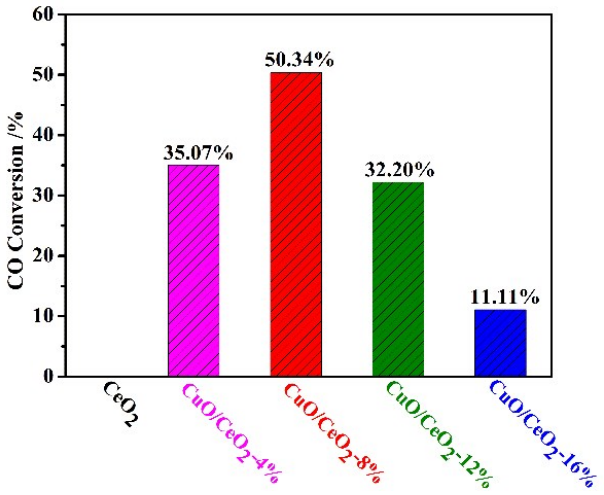


**Fig. S7** CO conversion at 110 °C for the bare $CeO_2$ and $CuO/CeO_2$-X% samples.

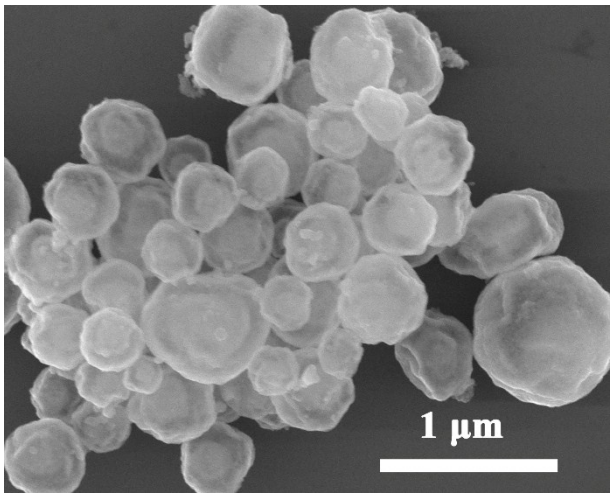


**Fig. S8** SEM image of $CuO/CeO_2$-8% after catalysis.

**Table S1** ICP analytical results of $CuO/CeO_2$-X% samples.

| samples | Cu (wt%) |
|---|---|
| $CuO/CeO_2$-4% | 4.11 |
| $CuO/CeO_2$-8% | 7.97 |
| $CuO/CeO_2$-12% | 11.44 |
| $CuO/CeO_2$-16% | 12.73 |

**Table S2** Textural (BET) characteristics of bare $CeO_2$ and $CuO/CeO_2$-X% samples.

| sample | BET Surface Area ($m^2/g$) | Pore Volume ($cm^3/g$) | Average Pore Size (nm) | Pore Size distribution |
|---|---|---|---|---|
| $CeO_2$ | 57.03 | 0.12 | 6.6 | 2-4 nm |
| $CuO/CeO_2$-4% | 32.36 | 0.14 | 10.3 | 2-4 nm |
| $CuO/CeO_2$-8% | 24.89 | 0.09 | 8.9 | 2-4 nm |
| $CuO/CeO_2$-12% | 22.66 | 0.07 | 7.1 | 2-4 nm |
| $CuO/CeO_2$-16% | 21.05 | 0.07 | 7.4 | 2-4 nm |

**Table S3** Relative contents of $Cu^+$ and $Ce^{3+}$ of $CuO/CeO_2$-8% sample before and after catalysis analyzed by XPS

| catalysts | $Cu^+$ (%) | $Ce^{3+}/(Ce^{3+}+Ce^{4+})$ (%) |
|---|---|---|
| $CuO/CeO_2$-8% (before) | 30.25 | 21.07 |
| $CuO/CeO_2$-8% (after) | 25.30 | 17.31 |

**Table S4** Dispersion and content of CuO, CO conversion and TOF values for $CuO/CeO_2$-X% catalysts.

| Catalysts | $D_{CuO}$[a] (%) | Cu[b] (wt %) | CuO (wt %) | CO Conversion[c] (%) | TOF ($s^{-1}$)[d] |
|---|---|---|---|---|---|
| $CuO/CeO_2$-4% | 63.42 | 4.11 | 4.89 | 8.28 | $1.58 \times 10^{-3}$ |
| $CuO/CeO_2$-8% | 43.33 | 7.97 | 9.06 | 11.42 | $1.72 \times 10^{-3}$ |
| $CuO/CeO_2$-12% | 51.31 | 11.44 | 12.51 | 9.44 | $8.68 \times 10^{-4}$ |
| $CuO/CeO_2$-16% | 76.34 | 12.73 | 13.73 | 1.38 | $7.77 \times 10^{-5}$ |

[a]CuO dispersion ($D_{CuO}$) was determined by $H_2$-TPR + $N_2O$ chemisorption;[Ref. S1]

[b]Cu concentration determined by ICP-OES;

[c]Reaction temperature is 90 °C;

[d]TOF represents the turnover frequency calculated by equation (5).

**Table S5** Surface elemental composition of bare $CeO_2$ and $CuO/CeO_2$-X% determined by XPS.

| catalysts | Surface composition (at%) | | |
|---|---|---|---|
| | Cu 2p | Ce 3d | O 1s |
| $CeO_2$ | - | 25.85 | 74.15 |
| $CuO/CeO_2$-4% | 8.93 | 16.50 | 74.57 |
| $CuO/CeO_2$-8% | 10.25 | 17.80 | 71.95 |
| $CuO/CeO_2$-12% | 11.16 | 17.28 | 71.56 |
| $CuO/CeO_2$-16% | 12.06 | 18.28 | 69.66 |

**Table S6** Comparison of the activity for CO oxidation over different ceria-based catalysts.

| Catalysts | Morphology | Temperature (°C) with 100% CO Conversion | Reaction condition | References |
|---|---|---|---|---|
| $CuO/CeO_2$-8% | triple-shelled hollow nanospheres | 130 | 1%CO/21%$O_2$/78%$N_2$, 60000 mL·$g_{cat}^{-1}$·$h^{-1}$ | This work |
| $AuPd/CeO_2$ | multi-shelled hollow spheres | 145 | 1%CO/21%$O_2$/78%$N_2$, 30000 mL·$g_{cat}^{-1}$·$h^{-1}$ | Dalton Trans., 2017, 46, 1634-1644 |
| $Au@CeO_2$ | core-shell submicrospheres | 155 | 1%CO/1.6%$O_2$/97.4%He, 15000 mL·$g_{cat}^{-1}$·$h^{-1}$ | Energy Environ. Sci., 2012, 5, 8937-8941 |
| 20CuCe-L (copper-ceria) | Litchi-peel-like hierarchical hollow microspheres | 120 | 1%CO/10%$O_2$/89%Ar, 60000 mL·$g_{cat}^{-1}$·$h^{-1}$ | Nanoscale, 2018,10, 22775-22786 |
| 1CuCe-NR (copper oxide deposited on ceria) | nanorod | 122 | 1%CO/20%$O_2$/79%$N_2$, 80000 mL·$g_{cat}^{-1}$· $h^{-1}$ | ACS Catal., 2017, 7, 1313-1329 |
| $CuO@CeO_2$-50% | -- | 125 | 1%CO balanced in dry air, 20000 mL·$g_{cat}^{-1}$· $h^{-1}$ | J. Mater. Chem. A, 2017, 5, 13565-13572 |
| $CuO@CeO_2$-0.05 | spiny yolk@shell cubes | 120 | 1%CO/20%$O_2$/79%$N_2$, 60000 mL·$g_{cat}^{-1}$·$h^{-1}$ | Adv. Funct. Mater., 2018, 1802559 |
| $Au/CeO_2$@UiO-66 | core–shell microspherical beads | 100 | 1%CO/21%$O_2$/78%$N_2$, 120000 mL· $g_{cat}^{-1}$·$h^{-1}$ | J. Mater. Chem. A, 2017, 5, 13966-13970 |
| 300 °C-$CeO_2$-CuO | porous/hollow rod | 98 | 1%CO/10%$O_2$/89%$N_2$, 60000 mL·$g_{cat}^{-1}$·$h^{-1}$ | ACS Appl. Mater. Interfaces, 2017, 9, 39594-39601 |